The 2013 World Congress on
Advances in Nano, Biomechanics, Robotics, and Energy Research (ANBRE13)
Seoul, Korea, August 25-28, 2013

Tumoral acidic pH-responsive drug delivery system based on a novel photosensitizer-fullerene for chemo-photodynamic therapy

*Zhenzhong Zhang[1)], Jinjin Shi[2)], Yan Liu[3)] and Lei Wang[4)]

[1), 2), 3), 4)] *Zhengzhou University, Zhengzhou, PR China*
[1)] *zhangzz08@126.com*

ABSTRACT

Fullerene has shown great potential both in drug delivery and photodynamic therapy. Herein, we developed doxorubicin (DOX)-loaded PEI-derivatezed fullerene (C60-PEI-DOX) to facilitate combined chemotherapy and photodynamic therapy in one system, and DOX was covalently conjugated onto C60-PEI by pH-sensitive hydrazone linkage. The release of DOX from C60-PEI-DOX showed a strong dependence on pH values. Compared with free DOX in an in vivo murine tumor model, C60-PEI-DOX afforded higher antitumor efficacy without obvious toxic effects to normal organs owing to its good tumor targeting efficacy and 2.4-fold higer DOX released in tumor than in the other tissues. Besides, the ability of C60-PEI-DOX nanoparticles to combine the local specific chemotherapy with external photodynamic therapy significantly improved the therapeutic efficacy of cancer treatment. These results suggest C60-PEI-DOX may be promising for high treatment efficacy with minimal side effects in future therapy.

1. INTRODUCTION

The ultimate goal of cancer therapeutics is to increase the survival time and the quality of life of the patient by reducing the unintended harmful side-effects (Byrne *et al*. 2008). The most common cancer treatments are chemotherapy, radiation and surgery (Cai *et al*. 2010), with chemotherapy being the major treatment modality. Many therapeutic anticancer drugs, while pharmacologically effective in cancer treatment, are limited in their clinical applications due to their serious toxicities (Park *et al*. 2006). For example, doxorubicin (DOX) is one of the most effective drugs against a wide range of cancers. However, its clinical use is limited by severe side-effects such as cardio toxicity and acquired drug resistance (Han *et al*. 2012), which may be the cause of treatment failure in cancer (Pulkkinen *et al*. 2008). To overcome these obstacles, in recent years, with the development of cancer nanotechnology, researchers have focused on developing nano-scale anticancer drug carriers for improving therapeutic efficacy as well as reducing unwanted side effects (Kopecek 2003, Nishiyama *et al*. 2003, Hua *et al*. 2011). Fullerene (C60), the third allotrope of carbon after diamond and graphite, are nano-scale carbon materials with unique photo-, electro-chemical, physical properties

[1)] Professor
[2), 3), 4)] Graduate Student

and low systemic toxicity, having shown tremendous promise in target-specific delivery of drugs in the body (Montellano *et al*. 2011). However, their inherent hydrophobicity limit its use in biology, the employment of fullerenes for drug delivery is still at an early stage of development (Montellano *et al*. 2011), and up to now, there are only a few reports about fullerene derivatives being used for the delivery of anticancer drugs (Zakharian *et al*. 2005, Ashcroft *et al*. 2006). Recently, we reported a polyethylenimined fullerene (C60-PEI) which was modified with folic acid (FA) through an amide linker, then docetaxel was successfully encapsulated onto the C60-PEI-FA nanoparticles, and this C60 based drug delivery system afforded higher antitumor efficacy without obvious toxic effects to normal organs owing to its prolonged blood circulation and 7.5-fold higher DTX uptake of tumor (Shi *et al*. 2013).

Another great advantage of fullerene is its potential in photodynamic therapy (PDT) (Fan *et al*. 2012, Hu *et al*. 2012), PDT had been applied in the treatment of some malignant tumors, and it employed the activation of tumor-localizing photosensitizers (PS) by visible light which produced reactive oxygen species (ROS) leading to cytotoxic effect (Henderson *et al*. 2004). The absorption of visible light combined with an efficient intersystem crossing to a long-lived triplet state which makes fullerenes generate reactive oxygen species upon illumination and allow fullerenes to be photosensitizer (PS) (Markovic and Trajkovic 2008, Xiao *et al*. 2010). Due to the enormous PDT potential of fullerene, in recent years there has been much interest in studying possible biological activities of fullerenes with a view to using them in medicine (Milanesio *et al*. 2005), for example, malonic acid derivatives of C60 have a obvious photosensitive effect and significant cytotoxicity in vitro experiments (Isakovic *et al*. 2006). Sugar derivatives of C60 with high solubility can lead to death of cancer cells exposed to visible light (Mikata *et al*. 2003). In this work, PDT was also conducted in order to obtain a synergistic effect to B16-F10 cells and malignant tumor in C57 mice models by use of the C60 based drug delivery system.

The tumor metabolic profile is different within the interstitial matrix where poor oxygen perfusion causes elevated levels of lactic acid and a reduction in pH from 7.40 to about 6.00 (Gerweck and Seetharaman 1996, Qiu and Park 2001). These variations of pH in tumor tissues can be strategies for pH-sensitive drug delivery at local microenvironments due to not only decrease the side cytotoxicity but also promote the efficacy of chemotherapy. Over the past decade, pH-responsive biomaterial studies have attracted much attention. Guo et al. demonstrated that super paramagnetic nanocarriers with folate-mediated and pH-responsive targeting properties had obvious antitumor efficacy for Hela cells (Guo *et al*. 2011). The HA-DOX nano conjugate exhibits sustained release characteristic, reduces toxicity and inhibits breast cancer progression in xenografts of human breast cancer, leading to an increased survival rate (Cai *et al*. 2010). In general, a well-designed pH-responsive nano carrier should have a high loading efficiency and a long-term stability in the blood circulation, and should respond rapidly to an acidic pH stimulus and consequently release the drugs in the pathologic area (Gao *et al*. 2011). For pH-sensitive nano carrier–anticancer drug conjugates, various synthetic approaches have been adopted to include spacers such as acid-labile linkages between the nanoscale materials and drug. Hydrazone bond was such a kind of acid-labile linkages, which could quickly hydrolyze in acidic environment (pH < 7) like the tumor tissue, however it was stable in neutral environment (pH = 7.4) like the blood

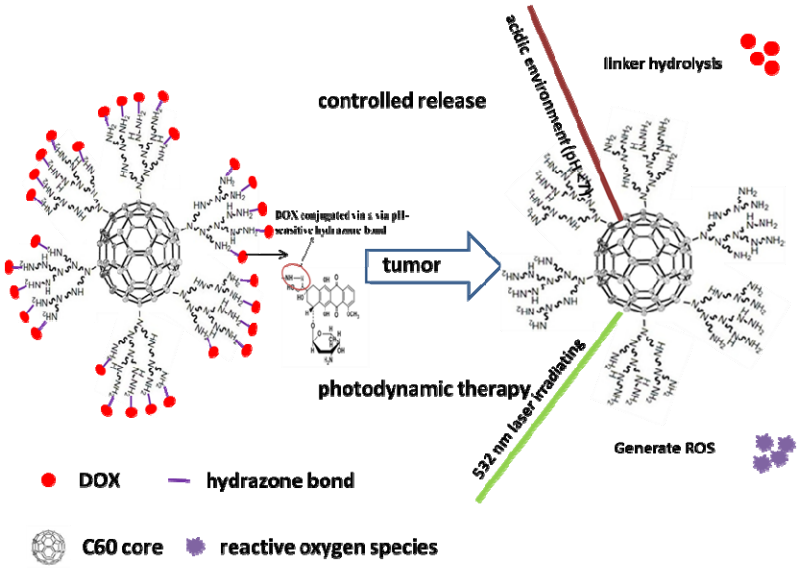

Fig. 1 Scheme of drug loading, pH-dependent released from C60-PEI-DOX and photodynamic therapy

(Etrych *et al*. 2001). Hydrazone bond was widely used in the pH-sensitive drug delivery. In this study, DOX was attached to C60 via hydrolytically degradable pH-sensitive hydrazone bonds to obtain a controlled release DOX delivery system.

In current study, a new DOX delivery system with the abilities of pH-sensitive and photodynamic therapy was designed, synthesized, characterized and explored its potential applications both in drug delivery and in photodynamic therapy. The drug delivery system was based on a polyethylenimined fullerene (C60-PEI) with high aqueous solubility, neutral pH and accessibility to further modification. PEI grafted onto the surface of C60 was a dendritic structure (Shi *et al*. 2013), and this dendritic structure could spread the pH-sensitive area, diminish the burst release, and increase drug loading capacity. DOX, which has been used extensively in the treatment of various cancers, was employed as the model drug and linked to PEI via 2 steps. First, a intermediate-carboxyl phenylhydrazine was reacted with carboxyl to form amide bonds and linked to the termini of branched PEI via primary amine bonds, after that, DOX was linked to carboxyl phenylhydrazine via hydrolytically degradable pH-sensitive hydrazone bonds. The DOX release rate and efficiency could be controlled by hydrazone bonds through changing the pH values. Herein, a controlled release DOX drug delivery system (C60-PEI-DOX) with photodynamic therapeutic activity (Fig. 1) was developed and characterized by transmission electron microscopy (TEM) and dynamic laser scattering (DLS), and its DOX release efficiency or its treatment effect was examined using mouse melanoma B16-F10 cells and melanoma tumor-bearing mice models.

2. MATERIALS AND METHODS

2.1 Materials

Fullerene (C60, purity > 95%) were purchased from Henan Fengyuan Chemicals Co. Ltd. Doxorubicin (DOX, 20120503, purity > 98%) was gotten from Beijing Yi-He Biotech Co. Ltd. Aziridine, ethylenediamine ($H_2NCH_2CH_2NH_2$), carboxyl phenylhydrazine (HBA), N-(3-dimethylamino propyl-N0-ethylcar-bodiimide) hydrochloride (EDC·HCl), and dimethyl sulfoxide (DMSO) were obtained from Sigma-Aldrich Co. LLC. Sulforhodamine B (SRB), RPMI 1640 cell culture medium, penicillin, streptomycin, fetal bovine serum (FBS), and heparin sodium were bought from Gibco Invitrogen. Quantum dots (CdSe/ZnS Qds) were supplied by WuHan Jiayuan Quantum Dots Co. Ltd. Other reagents were acquired from China National Medicine Corporation Ltd. The dialysis bags (MWCO=10, 000) were from Spectrum Laboratories Inc.

2.2 Synthesis of C60-PEI-DOX

C60-PEI was synthesized according to the procedure of our previous study (Shi ***et al***. 2013). In brief, ethylenediamine ($H_2NCH_2CH_2NH_2$, 40 ml) dissolved in ethanol-water mixture (ethanol: water = 5:1, 96 ml) was added dropwise to a stirring dry toluene solution (200 ml) containing C60 (200 mg) and NaOH (2.0 g). After stirring at room temperature under protection of Ar for 7 days, the mixture was evaporated and dried in vacuum at 60°C for 24 h, then purified by repeated rinsing with ethanol-water mixture (ethanol: water = 6:1) and filtrations. The resulting solid products were dried in vacuum at 60°C for 24 h. The above product (100 mg), concentrated HCl (20 *μ*l) and aziridine (1.0 ml) were added into dichloromethane (60 ml), stirred and refluxed at 40°C under protection of Ar for 24 h. C60-PEI was obtained by filtering and washing in order of CH_2Cl_2 10 times, methanol twice and deionized water several times. DOX attached to C60-PEI through hydrazone bond was then prepared according to the following steps. C60-PEI (50 mg) was suspended with HBA (50 mg) in a pH 7.4 phosphate buffered saline (PBS) solution (50 ml), EDC.HCl (80 mg), and NHS (35 mg) was then added. The mixture was allowed to react at room temperature for 48 h, after which the conjugate was precipitated using 200 ml of anhydrous ethanol, then the precipitated was purified by repeated rinsing with ethanol and filtrations to remove the unreacted reagents to obtain C60-PEI-HBA complex. The resulting solid products were dried in vacuum at 60°C for 24 h. The above product (50 mg) and DOX (100 mg) were added into dimethyl sulfoxide (DMSO, 50 ml), stirred at the room temperature in the dark for 24 h, and then dialyzed by a membrane (MWCO = 10, 000, Spectrum Laboratories Inc) for 3 days to remove free DOX and DMSO, finally the solution was freeze-dried to obtain the C60-PEI-DOX as a fine powder. The amount of DOX loaded onto C60-PEI was measured at 490 nm by UV-VIS spectrometer.

2.3 Characterization

DLS (Zetasizer Nano ZS-90, Malvern, UK) and TEM (Tecnai G2 20, FEI) were used for characterizing particle size, zeta potential and morphological of C60-PEI-DOX, respectively. The optical properties of C60-PEI and C60-PEI-DOX were characterized using an ultra-violet-visible (UV-VIS) spectrometer (Lambda35, Perkin-Elmer, USA). FT-IR spectra were recorded on a Nicolet iS10 spectrometer (Thermo).

2.4 Evaluation of pH sensitivity

The release studies were performed in a glass beaker at 37°C in acetate buffer (pH 5.5) and phosphate buffer (pH 7.4) solutions. First, 20 mg of C60-PEI-DOX was dispersed in 5 ml of water and placed in a dialysis bag (MWCO = 10, 000). The dialysis bag was then immersed in 45 ml of the release medium and kept in a horizontal laboratory shaker maintaining a constant temperature and stirring (100 rpm). Samples (2 ml) were periodically removed and the volume of each sample was replaced by the same volume of fresh medium. The amount of released DOX was analyzed with a spectrophotometer at 490 nm. The drug release studies were performed in triplicate for each of the samples.

2.5 Cell culture, cytotoxicity and phototoxicity assay

B16-F10 mice melanoma cell line was obtained from Chinese Academy of Sciences Cell Bank (Catalog No. TCM36). Cells were cultured in normal DMEM culture medium with 10% fetal bovine serum (FBS) and 1% penicillin/streptomycin in 5% CO_2 and 95% air at 37°C in a humidified incubator.

The cytotoxicity of C60-PEI-DOX against B16-F10 cells was assessed by using the standard SRB assay. The B16-F10 cells were cultured and lifted as described above before seeding (1×10^4) into 96-well plates and incubating for 24 h. The medium then was replaced with fresh medium containing various concentrations of free DOX, C60-PEI and C60-PEI-DOX for 24 h, the cells were or were not irradiated with 532 nm laser (Changchun laser research center) with the power density of 100 mW/cm^2 for 5 min.

2.6 Xenograft tumor mouse model

All animal experiments were performed under a protocol approved by Henan laboratory animal committee. Mice melanoma tumor models were generated by subcutaneous injection of 1×10^6 B16-F10 cells in 0.1 ml saline into the right shoulder of female C57 mice (18~22 g, Henan laboratory animal center). The mice were used when the tumor volume reached 60~100 mm^3 (~4 days after tumor inoculation).

2.7 In vivo antitumor effect

The mice were divided into five groups (six mice per group), minimizing the differences of weights and tumor sizes in each group. The mice were administered with (a) saline (0.1 ml), (b) C60-PEI/532 nm laser (5.6 mg/kg), (c) DOX (5 mg/kg), (d) C60-PEI-DOX (DOX dose: 5 mg/kg, C60-PEI dose: 5.6 mg/kg) and (e) C60-PEI-DOX/532 nm laser (DOX dose: 5 mg/kg, C60-PEI dose: 5.6 mg/kg) in saline were intravenous injected into mice via the tail vein every 2 days, respectively and then the tumor regions were irradiated with 532 nm laser (100 mW/cm^2, 5 min) at 3 h post-injection. The mice were observed daily for clinical symptoms and the tumor sizes were measured by a caliper every other day and calculated as the volume = (tumor length) × (tumor width)^2/2.

2.8 DOX release from C60-PEI-DOX in different tissues

The tumor-bearing mice were fasted but had access to water adlibitum for 12 h before killed, the main organs (heart, liver, spleen, lung, kidney and tumor) and blood were collected and weighed, after saline was added to each sample (saline weight: organ weight=1:1), the mixers were homogenized to obtain homogenate of different organs. 4 mg of C60-PEI-DOX was dispersed in 1 ml of water and placed in a dialysis bag (MWCO=10, 000). After 48 h, 500 μl homogenate was drawn, and the samples were added into a chloroform-methanol mixture (chloroform: methanol=4:1, 2 ml), and mixed by vortex, after centrifuged at 4000 rpm for 20 min, the chloroform layers were collected and then the concentrations of DOX were determined by high performance liquid chromatography (HPLC, 1100 Agilent, USA) with the following conditions: an Eclipse XDB-C18 column (150 mm × 4.6 mm, 5 *μ*m); mobile phase methanol: 0.01 mol/ml potassium dihydrogen phosphate: glacial acetic acid (68:31.5:0.5); column temperature 30°C; flow rate 1.0 ml/min; injection volume 40 *μ*l; and fluorescence detection wavelength: excitation wavelength (480 nm) and emission wavelength (550 nm) (Kim ***et al***. 2008). The studies were performed in triplicate for each of the samples.

2.9 Biodistribution studies

CdSe/ZnS (Qds 1.5 mM, 200 *μ*l) were added to C60-PEI-DOX nannosuspension (C60-PEI-DOX dose: 1 mg/ml, 3 ml), and stirred at room temperature in the dark for 12 h. The resulting product (C60-PEI-DOX-Qds) was obtained by repeating rinse with deionized water and filtrations. 0.2 ml of Qds and C60-PEI-DOX-Qds (with the same dose of Qds, confirmed by fluorescence spectra) were intravenous injected into tumor-bearing mice (3 mice per group). After injection for 3 h, the mice were killed to collect heart, liver, spleen, lung, kidney and tumor, then the collected tissues were made into frozen sections, and imaged by a Fluorescence Microscope (Zeiss LSM 510).

3. RESULT AND DISSICUSSION

3.1 Synthesis and characterization of C60-PEI-DOX

The inherent hydrophobicity limits the use of C60 in drug delivery, to overcome this obstacle, polyethylenimined fullerene (C60-PEI) with high aqueous solubility, neutral pH and accessibility to further modification, was synthesized. PEI-derivatezed was performed via a cationic polymerization of aziridine in the presence of amine-functionalized C60 (C60-NH_2), and C60-NH_2 was obtained by introducing ethylenediamine onto the surface of C60 (Fig. 2(A)). The analysis of TEM, FT-IR spectrum, and TGA showed that the functionalized process of C60-PEI was successful. (Details see our previous research (Shi ***et al***. 2013). The HBA molecules were reacted with carboxyl to form amide bonds and linked to the termini of branched PEI via primary amine bonds, then DOX was attached to HBA molecules with carbonyl via hydrolytically degradable pH-sensitive hydrazone bonds (Fig. 2(A)). Fig. 2(B) showed the FT-IR spectra of C60-PEI, C60-PEI-HBA and C60-PEI-DOX. It can be seen that PEI grafted to

C60 was confirmed by the strong C-N (~1108 cm^{-1}) vibrations, N-H (~1641 cm^{-1}, ~3406 cm^{-1}) vibrations and C-H (2924 cm^{-1}) vibrations of PEI (Fig. 2B, a) (Zhao *et al*. 2009, Chen *et al*. 2010). C60-PEI-HBA gave the extra peaks at amide I (~1659 cm^{-1}) vibrations, amide III (~1380 cm^{-1}) vibrations, -NH_2 bending (~1600 cm^{-1}) vibrations and N-N (~980 cm^{-1}) vibrations (Figs. 2(B) and (b)) (Park *et al*. 2006), indicating HBA was conjugated to C60-PEI. FT-IR results also showed that DOX conjugated to C60-PEI-HBA was confirmed by extra peaks of C60-PEI-DOX at (~1531 cm^{-1}) vibrations and (~1631 cm^{-1}) vibrations which were consistent with those expected for the hydrazone bond between hydrazine of C60-PEI-HBA and the DOX (Figs. 2(B) and (C)) (He *et al*. 2010).

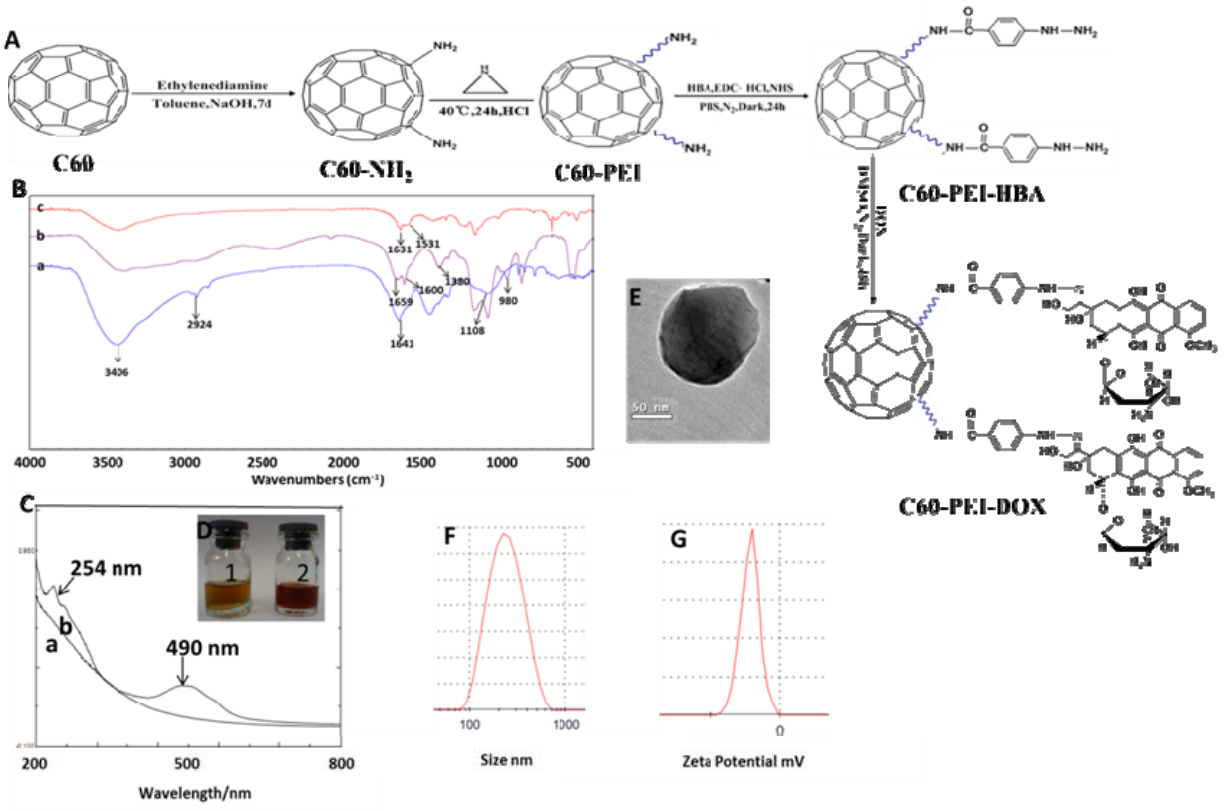

Fig. 2 Synthesis and characterization of C60-PEI-DOX: (A) schematic illustration of the synthetic steps for fullerene functionalization and conjugation of DOX; (B) FT-IR spectrum of (a) C60-PEI, (b) C60-PEI-HBA and c) C60-PEI-DOX; (C) UV spectrum of C60-PEI-DOX and C60-PEI solutions in water showing the doxorubicin absorption at 490nm; (D) solution of 1) C60-PEI and 2) C60-PEI-DOX in water. Transmission electron microscopy shows a (E) magnified image of a single C60-PEI-DOX aggregate; (F) and (G) Dynamic light scattering analysis of C60-PEI-DOX

We developed a fullerene-DOX (C60-PEI-DOX), and DOX was linked to C60-PEI through a hydrolytically degradable pH-sensitive hydrazone bonds. DOX attached to C60-PEI was also confirmed by a strong absorption peak at around 490 nm and 254 nm over C60-PEI background (Fig. 2(C)). C60-PEI-DOX was stable in water over multiple weeks without significant aggregation (Fig. 2(D)). DOX loading to the fullerene

nanostructures was quantified by absorption spectroscopy at 490 nm, and was found that DOX loading efficiency ~89.2% (weight ratio of DOX/C60-PEI), Such a value of loading was almost the same with carbon nanotubes (Wang *et al*. 2011, Murakami *et al*. 2004, Liu *et al*. 2007), which were always below 100wt%. This result indicated C60 was a promising material for drug delivery.

We found that C60-PEI-DOX tend to form monodisperse aggregates in the size range of 100~200 nm as confirmed by DLS and TEM. These could not be disintegrated into smaller individual fullerenes due to the intermolecular interactions, such as H-bonding. The size and zeta potential of C60-PEI-DOX were 181 ± 4.7 nm (Fig. 2(F)) and -21.7 ± 2.1 mV (Fig. 2(G)) respectively. TEM image of C60-PEI-DOX were shown in (Fig. 2(E)), which was consistent with the result of DLS. A pharmacokinetic standpoint as nanoparticles less than 5 nm have been reported to be cleared by kidney (Peer *et al*. 2007), while larger nanoparticles have been reported to preferentially home into tumors through leaky tumor neovasculature as a result of the enhanced permeability and retention (EPR) effect (Peer *et al*. 2007). The size of C60-PEI-DOX opened up the possibility of targeting tumors without being cleared rapidly by kidney.

3.2 Evaluation of pH sensitivity

The drug release behavior of C60-PEI-DOX nanoparticles was investigated under a simulated physiological condition (PBS, pH 7.4) and in an acidic environment (acetate buffer, pH 5.5) at 37°C to assess the feasibility of using C60-PEI-DOX as an anticancer drug delivery carrier. The drug release profiles of DOX from C60-PEI-DOX are shown in Fig. 3. This study clearly showed that the pH of the medium had a strong effect on the DOX release rate from C60-PEI-DOX nanopaticles. The DOX release from C60-PEI-DOX at pH 7.4 was considerably slow, with an initial burst of about 8.4%,and only 14.1% of the drug released after 60 h. This result suggests that C60-PEI-DOX maintained drug–nanocarrier interactions by the hydrazone linkage under physiological conditions. In mouse normal tissues, the releases of C60-PEI-DOX are slow too (Fig. 9). At pH 5.5, the DOX release rate was much faster, with approximately 86.2% of the drug

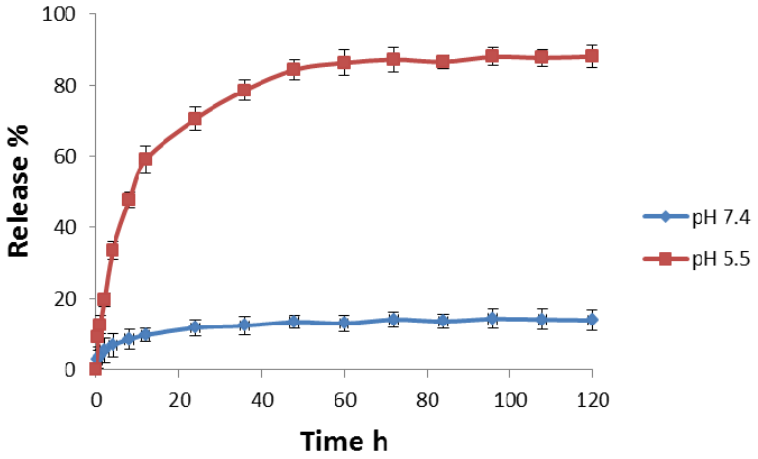

Fig. 3 Release profiles of DOX from C60-PEI-DOX at 37°C
*Note: Data are presented as mean ± standard deviation (n = 3)

released within 60 h. This result shows that the release of DOX from C60-PEI in an acidic environment was governed by the acid-cleavable characteristic of the hydrazone linkage between DOX molecules and the C60-PEI backbone. An acid-cleavable hydrazone linkage can undergo hydrolysis under acidic conditions; thus, DOX can be released from the C60-PEI by hydrolysis of the hydrazone linkage at the 13-keto position of DOX molecules. In the acidic medium, the release profile of DOX from C60-PEI-DOX showed a pseudo-saturation behavior after 60 h, this phenomenon can be attributed to the adsorption characteristics of C60. As the linkages of DOX and C60-PEI broke, the cleaved DOX released into the incubation medium, during the process, DOX was adsorbed to the core of C60. Therefore, a small portion of the cleaved DOX was physically adsorbed to C60, and this part of DOX could not release from C60-PEI. This pH-dependent releasing drug delivery system could withhold the drug in the plasma at normal physiological conditions (pH 7.4), thereby, greatly reducing the side effects to the normal tissues. However, a faster release occurs once C60-PEI-DOX reach the tumor site or are taken up by the tumor cells via an endocytosis process because the pH values of the tumor ranges from 4.5 to 6.5, which are much lower than the pH value of the normal physiological conditions (Gerweck and Seetharaman 1996, Kim *et al*. 2008), greatly improving the efficacy of cancer therapy.

3.3 Cytotoxicity and phototoxicity assay

All the cytotoxic effects studies against cultured B16-F10 cells were using the SRB assasy. The dark cytotoxicity study of C60-PEI on B16-F10 cells was carried out at different concentrations of C60-PEI in order to determin the systemic toxicity of the blank drug carrier. As shown in Fig. 4(a), cell viability remained above 85% even at the concentration up to 100 *μ*g/ml. This result indicated that C60-PEI was non-cytotoxic to B16-F10 cells after 24 h of incubation. B16-F10 cells were also incubated with different concentrations of free DOX, C60-PEI and C60-PEI-DOX for 24 h, the C60-PEI-DOX group has an equivalent DOX dosage to DOX group and an equal content of C60-PEI to C60-PEI group. Both the C60-PEI-DOX group and C60-PEI group were irradiated by 532 nm laser (100 mW/cm^2, 5 min). As seen from Fig. 4(b), a dose-dependent cytotoxicity of all groups was shown. According to the result, we can clearly see that C60-PEI exhibit a relatively small cytotoxic to B16-F10 cells, while C60-PEI/532 nm laser group greatly enhanced the cytotoxic, indicating C60-PEI is a promising photodynamic agent for cancer therapy (Liu and Tabata 2010, Hu *et al*. 2012). An advantage of photodynamic therapy is that can be positioned in the treatments (Zhao *et al*. 2012, Gandra *et al*. 2013), so in the in vivo antitumor study, we just irradiated tumor site, and that would reduce the side effects on normal tissues and organs. There is no significant difference between DOX and C60-PEI-DOX. At a DOX concentration of 0.5 *μ*g/ml, the inhibition rate of C60-PEI-DOX was 28.7%, indicating a higher cytotoxicity than C60-PEI/532 nm laser (3.2%) and C60-PEI-DOX/532 nm laser (26.8%). The lower cell-killing ability could be attributed to insufficient C60-PEI to producing enough ROS to kill cells for C60-PEI/532 nm laser group and C60-PEI-DOX/532 nm laser group. At a DOX concentration of 4 μg/ml, the inhibition rate of C60-PEI-DOX/532 nm laser group was significantly increased to 94.2%, while C60-PEI-DOX and C60-PEI/532 nm laser

were 63.4% and 60.2% respectively, indicating an enhanced cell-killing effect, thus, a synergistic therapeutic effect of PDT induced by C60 and DOX was observed on B16-F10 cells.

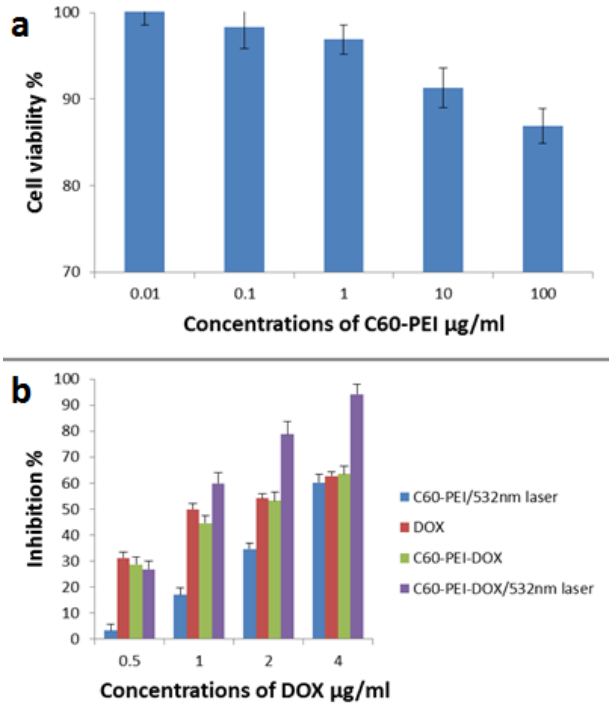

Fig. 4 Cytotoxicity and photocytotoxicity of (a) C60-PEI and (b) DOX, C60-PEI-DOX on B16-F10 cells.
*Note: Data are presented as mean ± standard deviation (n = 6)

3.4 Tumor growth inhibition in vivo

To investigate in vivo therapeutic efficacy of C60-PEI-DOX/532 nm laser, we conducted comparative efficacy studies. The B16-F10 tumor-bearing mice were divided into 5 groups and were treated with the protocols as summarized in method Section 2.7. The changes of relative tumor volume as a function of time were plotted in (Fig. 5a). After 10 days treatment, control group showed (V/V_0) of 11.27 ± 1.12, C60-PEI/532 nm laser vehicle showed (V/V_0) of 7.89±0.79, DOX and C60-PEI-DOX resulted in V/V_0 of 5.16 ± 0.81 and 3.78 ± 0.55, mice treated by C60-PEI/532 nm laser, DOX or C60-PEI-DOX had tumor growth inhibition (TGI) of 30.0%, 54.2% and 66.5%, respectively. The treatment C60-PEI-DOX/532 nm laser resulted in V/V_0 of 1.54 ± 0.42, representing a TGI of 86.3%, suggesting that it is significantly more effective than C60-PEI/532nm laser, DOX or C60-PEI-DOX ($p < 0.05$). Compared with the saline group, mice treated with C60-PEI/532nm laser, the tumor volume was reduced, this is a successful application that C60 was used as a photosensitizer in PDT to achieve in vivo tumor treatment efficacy. Because of the EPR effect (Oh *et al*. 2013, Shi *et al*. 2013), C60-PEI-DOX group could carry more DOX to the tumor site than DOX group, then the acid-cleavable hydrazone linkage can undergo hydrolysis in the tumor, so mice treated

only with DOX experienced a more rapid growth of tumor volume than C60-PEI-DOX. The growth of tumor tissue was successfully suppressed by C60-PEI-DOX/532 nm laser. This high therapeutic efficacy originates from the high DOX accumulation and ROS from C60 by 532 nm irradiation in tumor tissue. Overall, these results not only demonstrated that C60-PEI-DOX are highly useful for chemotherapy of tumors but also revealed that C60-PEI-DOX were powerful agents for combination chemotherapy with photodynamic therapy of cancer in vivo. Allowing for high toxicity usually leads to weight loss, we also measured the body weight of the mice for all groups during the treatments, free DOX resulted in a significant decrease in body weight of the animals over the experimental period, while in the C60-PEI-DOX-treated mice we observed an overall gain in body weight (Fig. 5(b)). These results indicated that C60-PEI-DOX increased the therapeutic index of the cytotoxic agent. Furthermore, C60-PEI-DOX can expectedly accumulate in the tumor tissues by escaping through the abnormally leaky tumor blood vessels, where hydrazone linkage hydrolysis release of the active drug, which can result in focal build-up of the active agent within the tumor resulting in reduced systemic toxic side effect of DOX (Chaudhuri *et al*. 2009).

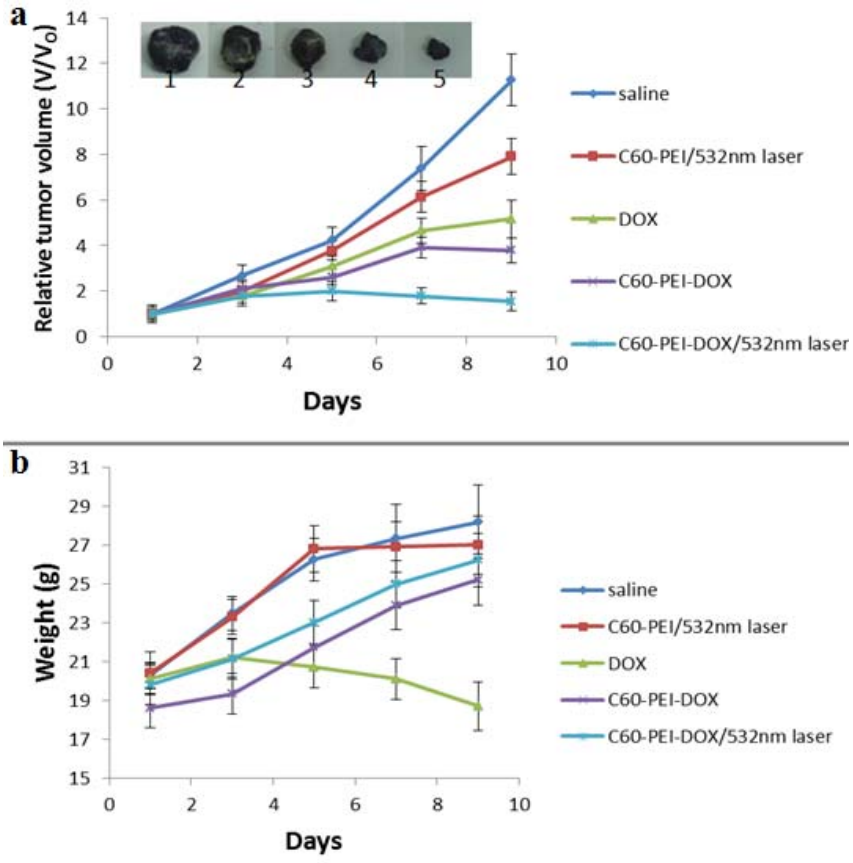

Fig. 5 (a) Average relative tumor volume (V/V_0) in a B16-F10 tumor-bearing mice model of treatment in vivo. Inset, a photo of representative tumors taken out of an untreated-mouse (1), a C60-PEI/532 nm laser-treated mouse (2), a DOX-treated mouse (3), a C60-PEI-DOX-treated mouse (4) and a C60-PEI-DOX/532 nm laser-treated mouse (5) after sacrificing the mice at the end of treatments; (b) Curves of mean body weight of mice receiving different treatments. Data are presented as mean ± standard deviation (n = 6)

3.5 DOX release from C60-PEI-DOX in different tissues

In order to investigate the DOX release from C60-PEI-DOX in vivo, we determined the DOX release in different tissues. The samples were treated with the protocols as summarized in method Section 2.8. The drug release profiles of DOX from C60-PEI-DOX in defferent tissues were shown in Fig. 6. This study clearly showed that the DOX release at blood, heart, liver, spleen, lung and kidney were considerably slow, and only below 24% of DOX released after 48 h. This result suggested that C60-PEI-DOX maintained DOX-nanocarrier interactions by the hydrazone linkage under the aboved tissues which had the physiological conditions. However, compared with the normal tissues, the DOX release at tumor was relatively faster, and 57.4±6.9% of DOX released after 48 h. This result indicated DOX could be released from C60-PEI-DOX by hydrolysis of the hydrazone linkage in tumor. A more DOX release from C60-PEI-DOX in tumor could be attributed to the acidic conditions of tumor site (Dong *et al*. 2010, Muhammad *et al*. 2011). We also found that more DOX released in normal tissues than that of in pH = 7.4 PBS buffer (Fig. 3), and this could arise from enzymatic releasing of the active drug. C60-PEI-DOX had the ability of selectively releasing of DOX in different tissues, and this ability greatly reducing the side effects to normal tissues and improving the efficacy of cancer therapy.

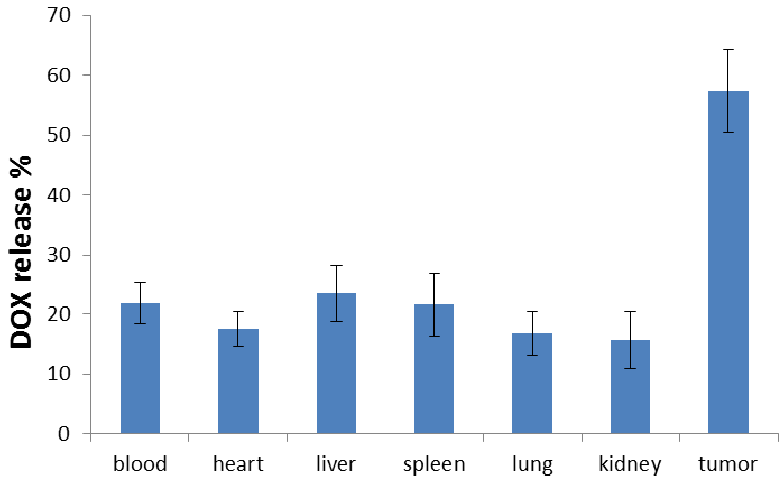

Fig. 6 DOX release from C60-PEI-DOX in different tissues for 48 h. Data are presented as mean ± standard deviation (n = 3)

3.6 Biodistribution of the C60-PEI-DOX

To further understand the antitumor efficacy of C60-PEI-DOX/532nm laser, We investigated the biodistributions of C60-PEI-DOX by injecting Qds labeled conjugates into tumor-bearing mice. After injection for 3 h, high uptakes of C60-PEI-DOX in the RES organs (liver/spleen) and tumors were observed (Kubota, Tahara *et al*. 2011) (Fig. 7). The result showed that C60 nanoparticles can server as drug carriers for the targeted drug delivery to the tumor site due to the EPR effect, and this resulted in higher level of

ROS induced by C60 under 532 nm laser irradiation and cleaved DOX accumulations in tumor site, thus improving cancer therapeutic effect and reducing the nonspecific side effects of anticancer agents. The ability of higher DOX and photosensitizer delivery efficiency to tumor by C60-PEI-DOX was striking and directly responsible for the higher tumor suppression efficacy of C60-PEI-DOX/532 nm laser than the other groups. Although, C60-PEI-DOX/Qds group showed higher fluorescence intensities of Qds in liver, spleen and lung tissues, DOX was still maintained in C60-PEI-DOX nanoparticles by the hydrazone linkage, and the toxicity of DOX had not been demonstrated. This result was also confirmed by the H&E staining results.

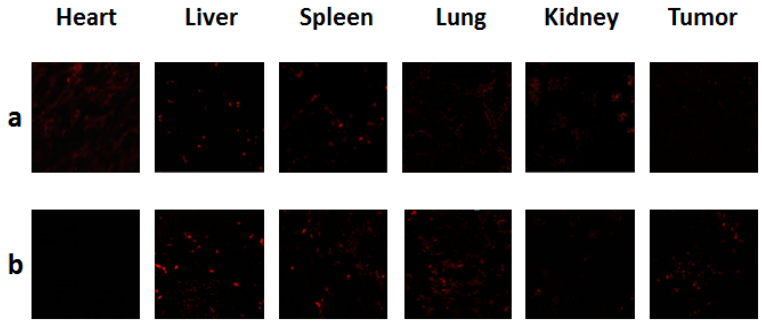

Fig. 7 The distributions of tumor-bearing mice. Fluorescence images of
(a) Qds alone; and (b) C60-PEI-DOX-Qds in major organs and tumor of mice (200×)

4. CONCLUSIONS

In summary, a pH-sensitive drug delivery system (C60-PEI-DOX) was successfully synthesized, and the release of DOX from C60-PEI-DOX depended strongly on the pH values. It was found that DOX released rapidly at acidic pH's such as those encountered in tumor tissue due to the hydrolysis of hydrazone linkage. We have studied the theapeutic effects of C60-PEI-DOX both in vivo and in vitro, which could be used for chemo-photodynamic therapy. The combined treatment resulted in a higher suppression of tumor growth in a cultured B16-F10 cells in vitro and in a murine melanoma cancer model in vivo with minimal side effects. These results indicated that C60-PEI-DOX could provide passive tumor targeting abilities, controlled drug release and a synergistic effect with photodynamic therapy, thereby, C60-PEI-DOX was a promising nanomedicine for cancer therapy.

5. ACKNOWLEDGEMENTS

The work is supported by grants from the National Natural Science Foundation of China (Nos. 3097/3660). The authors gratefully acknowledge the support of K.C. Wang Education Foundation, Hong Kong.

REFERENCES

Ashcroft, J.M., D.A. Tsyboulski, *et al*. (2006), “Fullerene (C60) immunoconjugates: interaction of water-soluble C60 derivatives with the murine anti-gp240 melanoma antibody." Chem Commun (Camb), **28**, 3004-3006.

Byrne, J.D., T. Betancourt, *et al*. (2008), “Active targeting schemes for nanoparticle systems in cancer therapeutics”, *Adv*. *Drug Deliv*. *Rev*., **60**(15), 1615-1626.

Cai, S., S. Thati, *et al*. (2010), “Localized doxorubicin chemotherapy with a biopolymeric nanocarrier improves survival and reduces toxicity in xenografts of human breast cancer”, *J*. *Control Release*, **146**(2), 212-218.

Chaudhuri, P., A. Paraskar, *et al*. (2009), “Fullerenol-cytotoxic conjugates for cancer chemotherapy”, *ACS Nano*, **3**(9), 2505-2514.

Chen, M.L., X.W. Chen, *et al*. (2010), “Functionalization of MWNTs with hyperbranched PEI for highly selective isolation of BSA”, *Macromol*. *Biosci*., 10(8), 906-915.

Dong, L., S. Xia, *et al*. (2010), “A pH/enzyme-responsive tumor-specific delivery system for doxorubicin”, *Biomater*., **31**(24), 6309-6316.

Etrych, T., M. Jelinkova, *et al*. (2001), “New HPMA copolymers containing doxorubicin bound via pH-sensitive linkage: Synthesis and preliminary in vitro and in vivo biological properties”, *J*. *Control Release*, **73**(1), 89-102.

Fan, J., G. Fang, *et al*. (2012), “Water-Dispersible Fullerene Aggregates as a Targeted Anticancer Prodrug with both Chemo- and Photodynamic Therapeutic Actions”, *Small*, **9**(4), 613-621.

Gandra, N., G. Abbineni, *et al*. (2013), “Bacteriophage bionanowire as a carrier for both cancer-targeting peptides and photosensitizers and its use in selective cancer cell killing by photodynamic therapy”, *Small*, **9**(2), 215-221.

Gao, G.H., J.W. Lee, *et al*. (2011), “pH-responsive polymeric micelle based on PEG-poly(beta-amino ester)/(amido amine) as intelligent vehicle for magnetic resonance imaging in detection of cerebral ischemic area”, *J*. *Control Release*, **155**(1), 11-17.

Gerweck, L.E. and K. Seetharaman (1996), “Cellular pH gradient in tumor versus normal tissue: potential exploitation for the treatment of cancer”, *Cancer Res*., **56**(6), 1194-1198.

Gillies, E.R. and J.M. Frechet (2005), “pH-Responsive copolymer assemblies for controlled release of doxorubicin”, *Bioconjug*. *Chem*., **16**(2), 361-368.

Guo, M., C. Que, *et al*. (2011), “Multifunctional superparamagnetic nanocarriers with folate-mediated and pH-responsive targeting properties for anticancer drug delivery”, *Biomater*., **32**(1), 185-194.

Han, M., Q. Lv, *et al*. (2012), “Overcoming drug resistance of MCF-7/ADR cells by altering intracellular distribution of doxorubicin via MVP knockdown with a novel siRNA polyamidoamine-hyaluronic acid complex”, *J*. *Control Release*, **163**(2), 136-144.

He, Y., Y. Zhang, *et al*. (2010), “Dual-response nanocarrier based on graft copolymers with hydrazone bond linkages for improved drug delivery”, *Colloid*. *Surf*. *B Biointerface*, **80**(2), 145-154.

Henderson, B.W., S.O. Gollnick, *et al*. (2004), “Choice of oxygen-conserving treatment regimen determines the inflammatory response and outcome of photodynamic therapy of tumors”, *Cancer Res*., **64**(6), 2120-2126.

Hu, Z., C. Zhang, *et al*. (2012), “Photodynamic anticancer activities of water-soluble C(60) derivatives and their biological consequences in a HeLa cell line”, *Chem*. *Biol*. *Interact*, **195**(1), 86-94.
Hua, M. Y., H. W. Yang, *et al*. (2011), “Superhigh-magnetization nanocarrier as a doxorubicin delivery platform for magnetic targeting therapy”, *Biomater*., **32**(34), 8999-9010.
Isakovic, A., Z. Markovic, *et al*. (2006), “Inactivation of nanocrystalline C60 cytotoxicity by gamma-irradiation”, *Biomater*., **27**(29), 5049-5058.
JungWooPark, EunH.Chae, *et al*. (2006), “Preparation of fine N ipowders from nickel hydrazine complex”, *Mater*. *Chem*. *Phys*., **97**, 371-378.
Kim, D., E. S. Lee, *et al*. (2008), “Doxorubicin loaded pH-sensitive micelle: Antitumoral efficacy against ovarian A2780/DOXR tumor”, *Pharm*. *Res*., **25**(9), 2074-2082.
Kopecek, J. (2003), “Smart and genetically engineered biomaterials and drug delivery systems”, *Eur*. *J*. *Pharm*. *Sci*., **20**(1), 1-16.
Kubota, R., M. Tahara, *et al*. (2011), “Time-dependent variation in the biodistribution of C(6)(0) in rats determined by liquid chromatography-tandem mass spectrometry”, *Toxicol*. *Lett*., **206**(2), 172-177.
Liu, J. and Y. Tabata (2010), “Photodynamic therapy of fullerene modified with pullulan on hepatoma cells”, *J*. *Drug Target*, **18**(8), 602-610.
Liu, Z., X. Sun, *et al*. (2007), “Supramolecular chemistry on water-soluble carbon nanotubes for drug loading and delivery”, *ACS Nano*, **1**(1), 50-56.
Markovic, Z. and V. Trajkovic (2008), “Biomedical potential of the reactive oxygen species generation and quenching by fullerenes (C60)”, *Biomaterials*, **29**(26), 3561-3573.
Mikata, Y., S. Takagi, *et al*. (2003), “Detection of 1270 nm emission from singlet oxygen and photocytotoxic property of sugar-pendant 60 fullerenes”, *Bioorg*. *Med*. *Chem*. *Lett*., **13**(19), 3289-3292.
Milanesio, M. E., M. G. Alvarez, *et al*. (2005), “Porphyrin-fullerene C60 dyads with high ability to form photoinduced charge-separated state as novel sensitizers for photodynamic therapy”, *Photochem*. *Photobiol*., **81**(4), 891-897.
Montellano, A., T. Da Ros, *et al*. (2011), “Fullerene C(6)(0) as a multifunctional system for drug and gene delivery”, *Nanoscale*, **3**(10), 4035-4041.
Muhammad, F., M. Guo, *et al*. (2011), “pH-Triggered controlled drug release from mesoporous silica nanoparticles via intracelluar dissolution of ZnO nanolids”, *J*. *Am*. *Chem*. *Soc*., **133**(23), 8778-8781.
Murakami, T., K. Ajima, *et al*. (2004), “Drug-loaded carbon nanohorns: Adsorption and release of dexamethasone in vitro”, *Mol*. *Pharm*., 1(6), 399-405.
Nishiyama, N., S. Okazaki, *et al*. (2003), “Novel cisplatin-incorporated polymeric micelles can eradicate solid tumors in mice”, *Cancer Res*., **63**(24), 8977-8983.
Oh, K.S., H. Lee, *et al*. (2013), “The multilayer nanoparticles formed by layer by layer approach for cancer-targeting therapy”, *J*. *Control*. *Release*, **165**(1), 9-15.
Peer, D., J. M. Karp, *et al*. (2007), “Nanocarriers as an emerging platform for cancer therapy”, *Nat*. *Nanotechnol*., **2**(12), 751-760.
Prabaharan, M., J.J. Grailer, *et al*. (2009), “Amphiphilic multi-arm-block copolymer conjugated with doxorubicin via pH-sensitive hydrazone bond for tumor-targeted drug delivery”, *Biomaterials*, **30**(29), 5757-5766.

Pulkkinen, M., J. Pikkarainen, *et al*. (2008), “Three-step tumor targeting of paclitaxel using biotinylated PLA-PEG nanoparticles and avidin-biotin technology: Formulation development and in vitro anticancer activity”, *Eur*. *J*. *Pharm*. *Biopharm*., 70(1), 66-74.
Qiu, Y. and K. Park (2001), “Environment-sensitive hydrogels for drug delivery,” *Adv*. *Drug*. *Deliv*. *Rev*., **53**(3), 321-339.
Shi, J., H. Zhang, *et al*. (2013), “EI-derivatized fullerene drug delivery using folate as a homing device targeting to tumor”, *Biomaterials*, **34**(1), 251-261.
Wang, L., M. Zhang, *et al*. (2011), “Synergistic enhancement of cancer therapy using a combination of docetaxel and photothermal ablation induced by single-walled carbon nanotubes”, *Int*. *J*. *Nanomedicine*, **6**, 2641-2652.
Xiao, L., H. Aoshima, *et al*. (2010), “The effect of squalane-dissolved fullerene-C60 on adipogenesis-accompanied oxidative stress and macrophage activation in a preadipocyte-monocyte co-culture system”, *Biomaterials*, **31**(23), 5976-5985.
Yoo, H.S., E.A. Lee, *et al*. (2002), “Doxorubicin-conjugated biodegradable polymeric micelles having acid-cleavable linkages”, *J*. *Control*. *Release*, **82**(1), 17-27.
Zakharian, T. Y., A. Seryshev, *et al*. (2005), “A fullerene-paclitaxel chemotherapeutic: synthesis, characterization, and study of biological activity in tissue culture”, *J*. *Am*. *Chem*. *Soc*., **127**(36), 12508-12509.
Zhao, L., H. Chen, *et al*. (2009), “[Platinum tetrachloride coupled PEG-PEI as drug carrier and gene delivery vector]”, Zhejiang Da Xue Xue Bao Yi Xue Ban, **38**(1), 59-66.
Zhao, T., X. Shen, *et al*. (2012), “Gold nanorods as dual photo-sensitizing and imaging agents for two-photon photodynamic therapy”, *Nanoscale*, **4**(24), 7712-7719.